European Journal of Radiology 118 (2019) 175–180

Contents lists available at ScienceDirect

European Journal of Radiology

journal homepage: www.elsevier.com/locate/ejrad

Research article

Clinical usefulness of temporal subtraction CT in detecting vertebral bone metastases

Sodai Hoshiai[a,*], Tomohiko Masumoto[a], Shouhei Hanaoka[b], Yukihiro Nomura[c], Kensaku Mori[a], Tadashi Hara[a], Tsukasa Saida[a], Yoshikazu Okamoto[a], Manabu Minami[a]

[a] Department of Radiology, Faculty of Medicine, University of Tsukuba, 1-1-1 Tennodai, Tsukuba, Ibaraki, 305-8575, Japan
[b] Department of Radiology, The University of Tokyo Hospital, 7-3-1 Hongo, Bunkyo-ku, Tokyo, 113-8655, Japan
[c] Department of Computational Diagnostic Radiology and Preventive Medicine, The University of Tokyo Hospital, 7-3-1 Hongo, Bunkyo-ku, Tokyo, 113-8655, Japan

ARTICLE INFO

Keywords:
Subtraction technique
CT
Bone
Vertebra
Metastasis

ABSTRACT

Purpose: The purpose of this study was to determine whether temporal subtraction (TS) computed tomography (CT) contributes to the detection of vertebral bone metastases.

Method: The calculation of TS CT was composed of bony landmark detection, bone segmentation with a multiatlas-based method, and spatial registration. Temporal increase and decrease of the CT values were visualized in blue and red, respectively. Paired CT images of 20 patients with cancer and newly-developed vertebral metastases were analyzed. Control CT examinations of 20 different patients were also included. The presence of vertebral metastases on the TS CT was evaluated by two board-certified radiologists. Five additional board-certified radiologists and five radiology residents independently interpreted the 40 paired CT images with and without TS CT.

Results: In the lesion conspicuity evaluation, 96% of vertebral metastases were scored as excellent or good. In the image interpretation examination, according to free-response receiver operating characteristics analysis, the overall figure of merit (FOM) of the board-certified radiologist group was 0.892 and 0.898 with and without TS CT, respectively. The FOM of the resident group improved from 0.849 to 0.902 with viewing TS CT. In the subanalysis focusing on the location of the lesion, the FOM of the resident group significantly improved from 0.75 to 0.92 in vertebral arch lesions ($p = 0.001$).

Conclusions: The TS CT may be useful to detect vertebral metastases because almost all the vertebral metastases were shown to be favorable visualization. The TS CT was proven to be especially helpful for radiology residents in detecting vertebral arch metastases.

1. Introduction

The skeletal system is the third most frequent site for distant metastases, after the lungs and liver [1]. Bone metastases occurs in 50% of patients with cancer, and among these, 40–70% involve vertebral lesions [2]. Although vertebral metastases may initially be asymptomatic, neurological symptoms can occur due to vertebral compression fractures or spinal cord compression, resulting in deterioration of the quality of life [3,4]. Therefore, early and accurate detection of vertebral metastases before their occurrence is one of the most important responsibilities of radiologists in their routine practice.

Several approaches have been reported for the detection of bone metastasis. Although some researchers have proposed an automated computer-aided detection system for vertebral metastases using CT [5–7], vertebral arch lesions have not been sufficiently evaluated. Recently, Sakamoto et al. and Ueno et al. discussed the utility of the temporal subtraction (TS) CT method for the detection of bone metastasis. Although these authors were able to develop a sophisticated TS CT method to reduce artifacts caused by misregistration, the potential of TS CT has not been fully clarified [8,9]. In this study, we have assessed the clinical usefulness of temporal subtraction CT to aid radiologists in detecting vertebral bone metastases.

2. Materials and methods

This retrospective study was approved by our institutional review

Abbreviations: TS, temporal subtraction; JAFROC, jackknife free-response receiver operation characteristic; FOM, figure of merit; HU, hounsfield units

* Corresponding author.
E-mail address: hoshiai@md.tsukuba.ac.jp (S. Hoshiai).

https://doi.org/10.1016/j.ejrad.2019.07.024
Received 31 December 2018; Received in revised form 11 June 2019; Accepted 18 July 2019

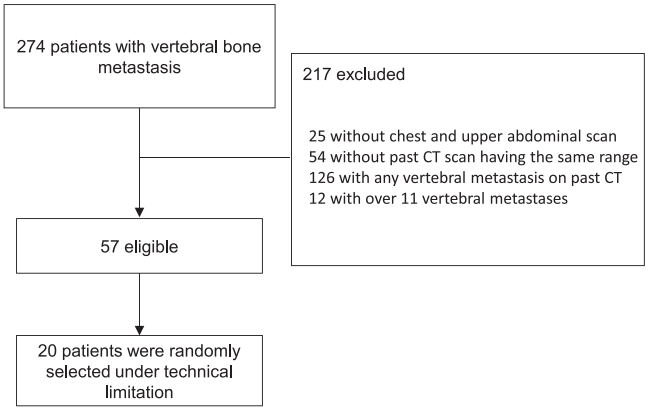

Fig. 1. A flowchart of the patient selection process.

board, and requirement for informed consent was waived.

2.1. Patients

Radiological records at our institute from June 2011 to October 2014 were searched for CT examinations associated with evident vertebral metastasis. CT scans covering at least the chest and upper abdomen were included regardless of whether a scan of the pelvis was included. Cases with past CT scans having the same scan range were included. Two board-certified radiologists (S.H. with 11 years of experience and T.M. with 23 years of experience) reviewed the paired current and past CT images and came to a consensus regarding the newly developed vertebral metastases in each patient. Cases exhibiting any vertebral metastasis in previous CT images were excluded from the study. One case that contained over 11 metastases was also excluded. Both post-contrast and non-contrast CT images were included in this study. The patient selection process is summarized in Fig. 1. The number of patients meeting the inclusion criteria was 57. Due to technical limitations, 20 patients were randomly selected among the 57 patients in order to reduce the number of patients. Finally, 20 patients with vertebral metastases were included as the metastases group in this study. Additionally, 20 other cancer patients without any vertebral metastases, but with at least one other organ metastasis, were included as a control group.

All patients were imaged in the supine position with a 16-, 64-, or 256- detector row CT system (IDT 16, Brilliance 64, or Brilliance iCT 256; Philips Medical Systems). Scans were obtained with the following parameters: 0.33, 0.5, or 0.75 s per rotation, 0.625 mm or 1.5 mm collimation, 0.5 to 0.9 pitch, and 120 kV. The electric current was automatically optimized following an acquisition of a scout image by a CT system program. All CT scans were reconstructed in the axial plane with a 2.0-mm thickness and a 2.0-mm interval.

2.2. Temporal subtraction (TS) CT

We developed a TS CT method that involves the detection of bony landmarks and bone segmentation with a multi-atlas-based method [10]. The entire spatial registration of the two-image series was automatically performed by a log-domain diffeomorphic Demons algorithm [11]. Details of the registration and segmentation algorithm are described elsewhere [12]. Temporal increases and decreases in the CT values were visualized using blue and red colors, respectively. The degree of saturation of the blue and red colors were determined by preliminary verification. The preliminary verification of the 6 osteoblastic lesions revealed a CT value increase ranging from 353 to 553, with the average being 432. The average CT value decrease of the 6 osteolytic lesions was 123, ranging from 49 to 233 in the preliminary verification. The changes in the CT values of the osteoblastic lesions were greater than those of the osteolytic lesions. The degree of blue color was proportional to the increase in CT value, and at 256 CT Hounsfield units (HU), the maximum value had been reached. The degree of red color was also proportional to the decrease in CT value and reached its maximum at 128 CT HU. The maximum values of both the blue and red colors in the lesions were determined by a board-certified radiologist (S.H.), who adjusted the degree of color to optimize visualization of bone metastases. The TS CT images were created from the calculated color maps and from the original CT images.

2.3. Conspicuity scoring of the vertebral metastases

Two board-certified radiologists (S.H. and T.M.) evaluated the conspicuity of the vertebral bone metastases on the TS CT images in the 20 patients. To evaluate the conspicuity of the lesion, a 3-point ordinal scoring system was used. Lesion conspicuity was scored as follows: excellent, when a lesion was easily distinguishable by vibrant colors; good, when a lesion was distinguishable by a weak color; and poor, when a lesion was not distinguishable due to scant coloration. In cases where a discrepancy existed between the two readers, a consensus was reached, and a final score was agreed upon.

2.4. Image interpretation examination

Two serial CT scans from 40 patients with malignant tumors were used for the image interpretation set as previously indicated. Of these patients, 20 had a newly developed vertebral bone metastasis and were thus included in the metastasis group. The remaining 20 patients did not present any vertebral bone metastases and were defined as the control group. Five board-certified radiologists (with 9, 15, 19, 21, and 24 years of experience) were asked to identify the vertebral bone metastases in the 40 patients. Five radiology residents also participated in this examination. Out of all the residents, four were in their third year of their residency training and one was in the fourth year of his residency. All CT images were viewed using a commercial software (Centricity RA1000: GE Healthcare, Barrington, IL). The readers were asked to mark the confidence level (1–100) of each lesion over 5 mm in size and to illustrate a simple schema of the lesion location to differentiate between vertebral body lesions and vertebral arch lesions. With respect to the lesions of the sacrum, metastases in the lateral and posterior parts were classified as the vertebral arch. Readers were allowed to adjust the window level and width and to browse the multiplanar reconstruction images. Reading sessions were conducted twice. The order of cases in each reading session was randomized. The readers were aware of the patients' sex, age, and primary cancer site but were not told the purpose of the examination. The first reading session was performed with the original paired CT images without the TS CT. The second reading session was performed at least 4 weeks after the first session. The second reading was conducted with the original CT images besides the axial and sagittal TS CT images. TS CT color images were supplied in a portable network graphics format files and viewed on a freely available graphic viewer (Irfanview 4.42, https://www.irfanview.com/). The reading time of each session was also recorded.

All results of the image interpretation examination were accessed by a board-certified radiologist (S.H.), who was not included among the readers. Classification of osteolytic or osteoblastic lesions were determined based on the dominant type of lesions.

2.5. Statistical analysis

Jackknife free-response receiver operation characteristic (JAFROC) analysis was applied for statistical assessment (freely available software, JAFROC 4.2.1 with random readers and random cases models, http://www.devchakraborty.com/) to compare the differences in the reading score between the sessions with and without TS CT in the image interpretation examinations [[13,14]]. JAFROC is one of the statistical

methods applied for lesion localization and for evaluation of the presence of multiple true positives per case, unlike conventional receiver operation characteristic analysis. Sub-analyses of the vertebral body, vertebral arch, osteolytic, and osteoclastic lesions were also independently assessed using JAFROC analysis. The score of the image interpretation examinations was presented as the figure of merit (FOM), which is equivalent of area under the receiver operating characteristic curve.

Other statistical analyses were performed using SPSS for Windows version 25 (IBM SPSS Inc., Chicago, IL). The male-female ratios of the patients were analyzed by using a Fisher's exact test, and the ages and the time intervals of the paired CT scans of the patients were analyzed by a Mann-Whitney U test. The numbers of assessed vertebral bones were also analyzed by using a Mann-Whiney U test. The Wilcoxon signed rank test was used to compare statistical differences in the reading time between both reading groups. Interobserver agreement was assessed by Kappa statistics. P values less than 0.05 were considered statistically significant.

3. Result

3.1. Characteristics of the patients

The characteristics of the patients are summarized in Table 1. The male-female ratio, age, and interval time of the paired CT scans were not significantly different between the metastases and the control groups. The total number of assessed vertebral bones were 379 and 368 in the metastases and the control group, respectively. In the metastases group, the assessed vertebral bones consisted of 46 cervical, 240 thoracic, 93 lumbar vertebral bones, and 16 whole sacra. The assessed vertebral bones in the control group consisted of 35 cervical, 240 thoracic, and 93 lumbar vertebral bones and 14 whole sacra. The average number of assessed vertebral bones per case was 19.0, ranging from 16 to 24 in the metastases group. The average number of assessed vertebral bones per case was 18.4, ranging from 16 to 23 in the control group. The number of assessed vertebral bones was not significantly different between the metastases and control groups.

The number of post-contrast CTs was 15 in the current CT image series in the metastases group. In the past CT image series, post-contrast CT was achieved in 16 patients belonging to the metastases group. Two pairs of past post-contrast and current non-contrast CT sets and a pair of past non-contrast and current post-contrast CT set were included in the metastases group. In the control group, a post-contrast CT was achieved in all patients in the past CT series. In the current CT series, a post-contrast CT was achieved in all control patients except 1.

Fifty-six vertebral metastases were identified in 20 patients. The average number of vertebral metastases per case was 2.85, ranging from 1 to 10 per patient. The lesions were classified based on location and included 44 vertebral body and 12 vertebral arch lesions. The metastases were also classified into 17 osteoblastic and 39 osteolytic lesions. The primary tumors in the metastases group consisted of four lung, four colon, three kidney, two ovary, two liver, one bladder, one uterus, one stomach, one breast, and one skin cancer. In the control group, six lung, four stomach, three esophageal, three pancreatic, two colon, two ovary, one duodenal, and one gall bladder cancer were recorded. Two patients in the control group had two primary forms of cancer.

Table 1
Characteristics of the patients.

	Metastases group	Control group	P value
Male : Female	10 : 10	14 : 6	0.333 [a]
Age (years)	64.1 ± 8.1	67.2 ± 10.6	0.157 [b]
Interval time of scans (days)	318 ± 377	199 ± 154	0.327 [b]
Number of assessed vertebral bones	19.0 ± 1.8	18.4 ± 1.4	0.142 [b]

Data are means ± standard deviations, a: Fisher's exact test, b: Mann-Whitney U test.

3.2. Conspicuity scoring of the vertebral metastases

The TS CT images were successfully created for all of the cases examined. Representative TS CT images are shown in Fig. 2 (see also Video, Supplementary data 1 and 2, which show sequential axial and sagittal images of TS CT, respectively). Osteolytic and osteoblastic metastases are shown in Fig. 2 and are red and blue in color, respectively. The evaluated score was excellent in 44 out of 56 metastases, good in 8, and poor in 4 cases according to reader 1. The score was excellent in 40 of 56 metastases, good in 13, and poor in 3 cases according to reader 2. The agreement rate between the two readers was favorable ($\kappa = 0.69$). The final scores based on their consensus were excellent in 41 of 56 metastases (73%), good in 13 (23%), and poor in 2 (4%) (Fig. 3).

3.3. Image interpretation examination

The FOM analyzed by the JAFROC is summarized in Tables 2 and 3 and Fig. 4. Overall, the FOMs of the experienced radiologist group were 0.892 and 0.898 with and without TS CT, respectively. Overall, the FOM of the resident group improved from 0.849 to 0.902 using TS CT; however, there was no statistical significance between the two groups ($p = 0.083$). In the sub-analysis focusing on the location of the lesion, the value of the FOM of the vertebral body was not significantly different between the experienced radiologist and resident groups. However, in the sub-analysis of the lesions in the vertebral arch, the FOM value significantly improved from 0.755 to 0.922 ($p = 0.001$) with TS CT in the resident group. The FOM of the lesions in the vertebral arch in the experienced radiologist group improved from 0.887 to 0.907. However, these values were not significantly different. Sub-analysis of the attenuation changes of the vertebral metastases, including osteoblastic and osteoclastic lesions, did not show any significant differences after the use of the TS CT in both experienced radiologist and resident groups.

Focusing on each vertebral metastasis, the average confidence rate is shown in Table 4. The total average confidence rating of the readers improved from 67.9% to 79.2% and 54.0% to 70.7%, using TS CT in the experienced radiologist and resident groups, respectively. Notably, the average confidence rating for the vertebral arch lesions remarkably improved from 60.9% to 77.3% and 41.6% to 70.3% using TS CT in the experienced radiologist and resident groups, respectively (Fig. 5).

The average reading time per case decreased from 4.2 to 4.1 min by using the TS CT in the experienced radiologist group. Additionally, in the resident group, the average reading time decreased from 4.6 to 3.7 min. However, these values were not statistically different.

4. Discussion

Early and accurate detection of vertebral bone metastases is very important. Even in patients with terminal stage cancers, vertebral bone metastasis may strongly affect their quality of life, since the they may cause a compression of the spinal cord, paralyzing their extremities. Although CT is the routinely used modality for the detection of cancer recurrence or metastasis during a follow-up survey, the sensitivity and specificity of vertebral bone metastases are not adequately high [15]. MRI or ^{18}FDG-PET are superior to CT for the detection of vertebral bone metastases; however, there are disadvantages to both MRI and ^{18}FDG-PET in terms of convenience and associated cost [16]. Therefore, it is diagnostically valuable to improve the detection ratio of bone metastasis using CT.

In this study, the TS CT method was developed for patients with cancers, with the aim of precisely localizing vertebral bone metastases. In the conspicuity evaluation of the TS CT, the agreement rate between

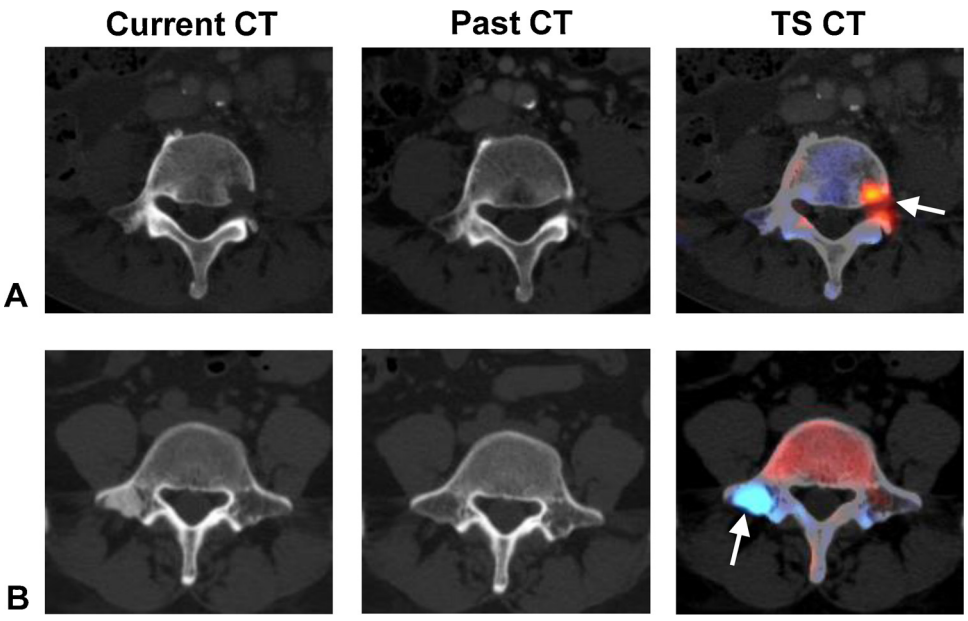

Fig. 2. Original current and past CT images and temporal subtraction (TS) CT images calculated by using the current and past CT images. A, A small osteolytic metastasis in the left posterior vertebral body using the current CT is obvious and appears as a red lesion in the TS CT (arrow). B, A newly developed osteoblastic metastasis is apparent in the TS CT and appears as a blue colored lesion (arrow).

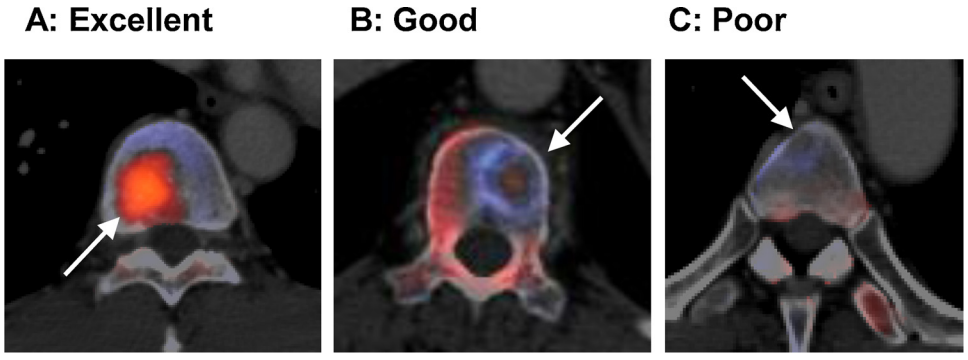

Fig. 3. Conspicuity of the vertebral metastases on the temporal subtraction (TS) CT. A, Excellent visualization, A vertebral body metastasis is clearly delineated by a vibrant red color (arrow). B, Good visualization, A vertebral osteolytic metastasis is delineated by a weak color with a marginal blue color (arrow). C, Poor visualization, A peripheral vertebral metastasis is not clearly visualized and is indistinguishable due to scant coloration (arrow).

Table 2
Individual and overall FOM and reading time of both the experienced radiologist and resident groups.

		FOM		Reading time per case (minutes)	
		without TS CT	with TS CT	without TS CT	with TS CT
Experienced radiologists	1	0.854	0.808	2.9	3
	2	0.932	0.841	5.4	3.8
	3	0.894	0.952	4.6	6.9
	4	0.864	0.934	3.4	3.2
	5	0.943	0.922	4.9	3.8
Overall		0.898	0.892	4.2	4.1
Residents	6	0.790	0.888	2.6	2.5
	7	0.887	0.953	5.3	3.4
	8	0.904	0.879	3.4	3.5
	9	0.845	0.886	3.6	3.4
	10	0.821	0.903	8.3	5.6
Overall		0.849	0.902	4.6	3.7

FOM; figure of merit, TS CT; temporal subtraction CT.

the two readers was favorable. Ninety-six percent of vertebral bone metastases were scored as excellent or good in the TS CT images. Some cases of peripheral metastasis of the vertebral body could not be visualized clearly on the TS CT. This may be due to imprecise recognition of the vertebral bone border.

According to the JAFROC analysis, the overall FOM was not statistically different between the two reading sessions with and without TS CT in the experienced radiologist group. This may be due to the radiologists' excellent reading performance even without the TS CT (FOM 0.898). Additionally, the reading time required for board-certified radiologists to view only the vertebral bones was longer. The readers were required to view at least two monitors since the TS CT and the original CT images were being viewed by each individual using independent graphic software in the second reading session. Construction of an adequate reading system is needed to view and scroll TS CT images and original past and current CT images simultaneously. To investigate this issue further, we plan to build and mount an integrated platform consisting of image viewing software possessing these abilities [17]. The FOM improved from 0.849 to 0.902 with TS CT in the resident group; however, this difference was not significant. The FOM score of residents with the TS CT was almost equal to that of the experienced radiologists. Importantly, the FOM significantly improved by using TS CT from 0.755 to 0.922 in vertebral arch lesions in the resident group ($p = 0.001$). The TS CT was useful for the detection of a vertebral arch metastasis by the residents. The reading time was slightly decreased using the TS CT for both residents and experienced radiologists. However, these values were not significantly different. This may be due to an increase in the number of total images needed during the TS CT session.

Although the TS technique has been previously applied to various modalities, including chest radiography [18,19], chest CT [20], and bone scintigraphy [21], only a few previous studies examined its potential application for the detection of bone metastases using CT [8,9]. Sakamoto et al. were the first to discuss the usefulness of TS CT to detect bone metastases; however, their spatial registration of a pair of

Table 3
Overall, vertebral body, vertebral arch, and osteoblastic and osteolytic lesion FOM of the experienced radiologist and resident groups.

	Experienced radiologists			Residents		
	without TS CT	with TS CT	P value	without TS CT	with TS CT	P value
Overall (n = 56)	0.898	0.892	0.852	0.849	0.902	0.083
Vertebral body (n = 44)	0.924	0.899	0.360	0.874	0.894	0.529
Vertebral arch (n = 12)	0.887	0.907	0.704	0.755	0.922	0.001*
Osteoblastic (n = 17)	0.949	0.926	0.452	0.857	0.955	0.129
Osteolytic (n = 39)	0.901	0.901	0.999	0.857	0.897	0.273

FOM; figure of merit, TS CT; temporal subtraction CT.
* Statistically significant difference.

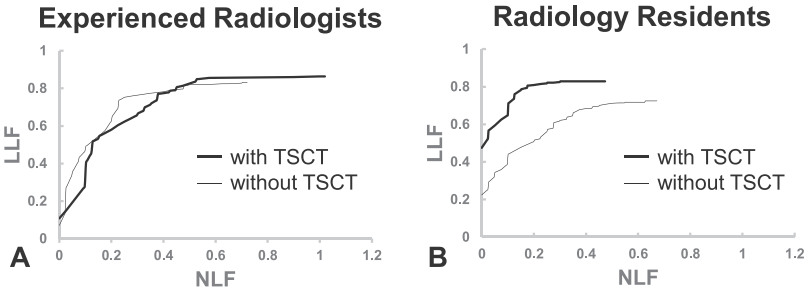

Fig. 4. Overall free-response receiver operator curves with (thick line) and without (thin line) temporal subtraction (TS) CT in both the experienced radiologist (A) and resident groups (B). Lesion detection is superior with TS CT in the radiology resident group. LLF; lesion localization fraction, NLF; non-lesion localization fraction.

Table 4
Average confidence rating of the experienced radiologist and the resident groups for the vertebral body, vertebral arch, and osteoblastic and osteolytic lesions.

	Experienced radiologists		Residents	
	without TS CT	with TS CT	without TS CT	with TS CT
Overall (n = 56)	67.9%	79.2%	54.0%	70.7%
Vertebral body (n = 44)	70.2%	78.4%	58.9%	68.2%
Vertebral arch (n = 12)	60.9%	77.3%	41.6%	70.3%
Osteoblastic (n = 17)	75.4%	86.3%	64.1%	80.8%
Osteolytic (n = 39)	65.1%	74.6%	51.3%	63.4%

TS CT; temporal subtraction CT.

CT images was semi-automatic, i.e., not fully automatic. Ueno et al. developed a fully spatial registration system of the CT images; however, they only assessed osteoblastic metastases. Our study is impactful and unique in that an automatic spatial registration of paired CT images was conducted, besides including both osteoblastic and osteoclastic lesions.

We acknowledge that our study has some limitations. First, vertebral metastasis was not verified pathologically, because all the patients with vertebral metastases did not undergo an aggressive treatment or an imaging test afterwards. For similar reasons, the false positive lesions pointed out by the readers were not truly proven as negative lesions. Second, we focused solely on vertebral metastases and did not include other bone metastases in this study. The rib, scapula, and pelvic bone were not eligible for assessment due to some misregistration of the positioning in a pair of CT images. Further studies exploring the ideal registration technique of the CT exams is needed. Third, the results of our study were derived from 40 patients comprising 20 vertebral bone metastases and 20 controls. Therefore, our results may not be applicable to other patients because of the small patient size and the retrospective study design. Moreover, because the 20 patients from the metastases group were randomly chosen from the 57 who were eligible to participate in the study, due to technical limitations, there may have been a selection bias. Finally, the contrast enhancement conditions in the current and past CT images were not identical across the metastases and control groups, which is a limiting factor of our study. However, contrast enhancement conditions are also not always identical in routine clinical practice.

In conclusion, we successfully reconstructed vertebral TS CT images from a pair of CT images, with a high reading agreement for conspicuity. Almost all the vertebral metastases were shown to be excellent or good depictions. Our study indicated that TS CT could be a useful tool for radiologists to detect vertebral bone metastasis, especially in detecting vertebral arch lesions for radiology residents.

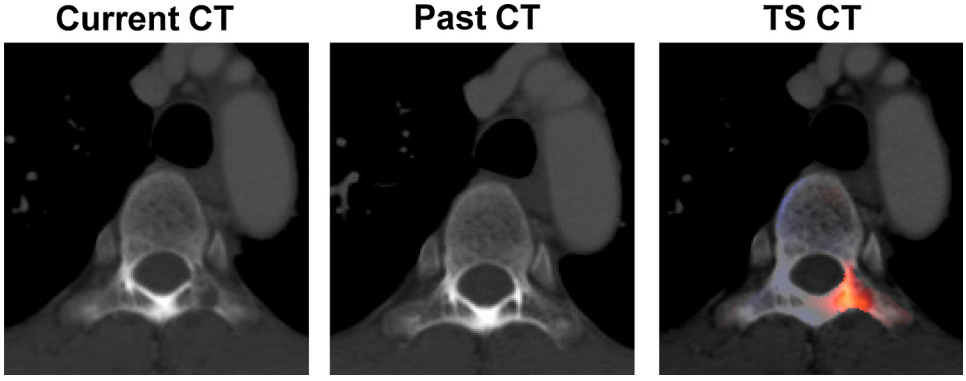

Fig. 5. An osteolytic metastasis on the left vertebral arch that could not be discerned in the original CT. The lesion becomes apparent in the TS CT. All of the experienced radiologists and 4 of the 5 residents did not provide any confidence ratings, indicating that the metastasis may be missed when viewing only the original CT image. Four out of 5 experienced radiologists and 4 out of 5 residents indicated a confidence rating of at least 74% for the detection of the metastasis using the TS CT image.

Funding

This work was supported in part by JSPS Grants-in-Aid for Scientific Research KAKENHI Grant Numbers 17H05282 and 18K12095.

Declaration of Competing Interest

We declare that we have no conflict of interest.

Acknowledgement

Takahiro Konishi, M.D., Yusuke Miyasaka M.D., Tetsuya Abe M.D., Shu Harada M.D., Sohta Masuoka M.D., Yohei Takei M.D. kindly participated as the readers in this study.

Appendix A. Supplementary data

Supplementary material related to this article can be found, in the online version, at doi:https://doi.org/10.1016/j.ejrad.2019.07.024.

References

[1] P.J. Boland, J.M. Lane, N. Sundaresan, Metastatic disease of the spine, Clin. Orthop. Relat. Res. 169 (1982) 95–102.
[2] C. Andreula, M. Murrone, Metastatic disease of the spine, Eur. Radiol. 15 (2005) 627–632.
[3] F. Bach, B.H. Larsen, K. Rohde, S.E. Børgesen, F. Gjerris, T. Bøge-Rasmussen, N. Agerlin, B. Rasmusson, P. Stjernholm, P.S. Sørensen, Metastatic spinal cord compression. Occurrence, symptoms, clinical presentations and prognosis in 398 patients with spinal cord compression, Acta Neurochir. 107 (1990) 37–43.
[4] D. Schiff, B.P. O'Neill, V.J. Suman, Spinal epidural metastasis as the initial manifestation of malignancy: clinical features and diagnostic approach, Neurology 49 (1997) 452–456.
[5] S.D. O'Connor, J. Yao, R.M. Summers, Lytic metastases in thoracolumbar spine:CAD at CT-preliminary study, Radiology 242 (2007) 811–816.
[6] J.E. Burns, Y. Jianhua, S. Tatjana, H.E. Muñoz, E.C. Jones, R.M. Summers, Automated detection of sclerotic metastases in the thoracolumbar spine at CT, Radiology 268 (2013) 69–78.
[7] M. Hammon, P. Danlerl, A. Tsymbal, et al., Automatic detection of lytic and blastic thoracolumbar spine metastases on computed tomography, Eur. Radiol. 23 (2013) 1862–1870.
[8] R. Sakamoto, M. Yakami, K. Fujimoto, K. Nakagomi, T. Kubo, Y. Emoto, T. Akasaka, G. Aoyama, H. Yamamoto, M.I. Miller, S. Mori, K. Togashi, Temporal subtraction of serial CT images with large deformation diffeomorphic metric mapping in the identification of bone metastases, Radiology 285 (2017) 629–639.
[9] M. Ueno, T. Aoki, S. Murakami, H. Kim, T. Terasawa, A. Fujisaki, Y. Hayashida, Y. Korogi, CT temporal subtraction method for detection of sclerotic bone metastasis in the thoracolumbar spine, Eur. J. Radiol. 107 (2018) 54–59.
[10] R.A. Heckemann, J.V. Hajnal, P. Aljabar, D. Rueckert, A. Hammers, Automatic anatomical brain MRI segmentation combining label propagation and decision fusion, Neuroimage 33 (2006) 115–126.
[11] T. Vercauteren, X. Pennec, A. Perchant, N. Ayache, Symmetric Log-domain diffeomorphic registration: a demons-based approach, in: D. Metaxas, L. Axel, G. Fichtinger, G. Székely (Eds.), Medical Image Computing and Computer-Assisted Intervention, Springer, New York, 2008, pp. 754–761.
[12] S. Hanaoka, Y. Masutani, M. Nemoto, Y. Nomura, S. Miki, T. Yoshikawa, N. Hayashi, K. Ohtomoa, A. Shimizu, Landmark-guided diffeomorphic demons algorithm and its application to automatic segmentation of the whole spine and pelvis in CT images, Int. J. Comput. Assist. Radiol. Surg. 12 (2017) 413–430.
[13] D.D. Dorfman, K.S. Berbaum, C.E. Metz, Receiver operating characteristic rating analysis. Generalization to the population of readers and patients with the jackknife method, Invest. Radiol. 27 (1992) 723–731.
[14] D.P. Chakraborty, K.S. Berbaum, Observer studies involving detection and localization: modeling, analysis, and validation, Med. Phys. 31 (2004) 2313–2330.
[15] R. Guillevin, J.N. Vallee, F. Lafitte, C. Menuel, N.M. Duverneuil, J. Chiras, Spine metastasis imaging: review of the literature, J. Neuroradiol. 34 (2007) 311–321.
[16] T. Liu, S. Wang, H. Liu, B. Meng, F. Zhou, F. He, X. Shi, H. Yang, Detection of vertebral metastases: a meta-analysis comparing MRI, CT, PET, BS and BS with SPECT, J. Cancer Res. Clin. Oncol. 143 (2017) 457–465.
[17] Y. Nomura, N. Hayashi, Y. Masutani, T. Yoshikawa, M. Nemoto, S. Hanaoka, S. Miki, E. Maeda, K. Ohtomo, CIRCUS: an MDA platform for clinical image analysis in hospitals, Trans. Mass-Data Anal. Images Signals 2 (2010) 112–127.
[18] J.M. Levy, S.J. Hessel, J.K. Crowe, Temporal subtraction chest radiography, Am. J. Roentgenol. 140 (1983) 823–824.
[19] S. Kakeda, K. Nakamura, K. Kamada, H. Watanabe, H. Nakata, S. Katsuragawa, K. Doi, Improved detection of lung nodules by using a temporal subtraction technique, Radiology 224 (2002) 145–151.
[20] H. Takao, I. Doi, T. Watanabe, M. Tateno, Temporal subtraction of thin-section thoracic computed tomography based on a 3-dimensional nonlinear geometric warping technique, J. Comput. Assist. Tomogr. 30 (2006) 283–286.
[21] J. Shiraishi, D. Appelbaum, Y. Pu, et al., Clinical utility of temporal subtraction images in successive whole-body bone scans: evaluation in a prospective clinical study, J. Digit. Imaging 680 (2011) 680–687.